Supporting Information

Mechanistic insights into selective and pH-independent removal of sulfamethazine by Fe_2O_3-functionalized lignin-derived biochar

Xueping Sun[a,1], Haitao Sheng[a,1], Xiaoyu Zhang[a,b,*], Xiangxue Chen[c], Xinbai Jiang[a], Cheng Hou[a], Jinyou Shen[a,b], Dan Chen[a,b,*]

[a]Key Laboratory of Environmental Remediation and Ecological Health, Ministry of Industry and Information Technology, School of Environmental and Biological Engineering, Nanjing University of Science and Technology, Nanjing 210094, China

[b]Engineering Research Centre of Chemical Pollution Control, Ministry of Education, School of Environmental and Biological Engineering, Nanjing University of Science and Technology, Nanjing 210094, China

[c]College of Biotechnology and Pharmaceutical Engineering, Nanjing Tech University, Nanjing 211816, China

Corresponding authors:

*Xiaoyu Zhang, E-mail: zhangxiaoyu1992@njust.edu.cn, TEL: 025-84315518

*Dan Chen, E-mail: danchen@njust.edu.cn, TEL: 025-84315518

Text S1. DFT Calculations and molecular electrostatic potential analysis

Theoretical calculations for SD, SMZ, and CAP were performed via Gaussian 16. Geometry optimizations were conducted at the M062X/def2-TZVPP level of theory. The structures of SD, SMZ, and CAP were fully optimized to ensure that the system energy corresponded to a minimum on the potential energy surface, as confirmed by vibrational frequency analysis, which revealed no imaginary frequencies. Following density functional theory (DFT) optimization, the molecular electrostatic potentials (MEPs) of the SDZ, SMZ, and CAP structures were subsequently calculated via Multiwfn (version 3.8) (Lu, 2024).

Text S2. HPLC analytical method

The residual SMZ concentration was quantified via high-performance liquid chromatography (HPLC; Thermo UltiMate 3000 HPLC) with a C18 column (250 mm × 4.6 mm, 5 μm) and DAD detector (λ = 275 nm). The mobile phase was methanol/water (30:70, v/v) at 1.0 mL/min.

Text S3. Desorption and regeneration experiments

The regeneration performance of Fe@LBC-800 was evaluated by desorbing SMZ at a solid/liquid ratio of 1:1 (mg/mL) at 35 °C and 180 rpm (Hu et al., 2024). Specifically, 0.125Fe@LBC-800 was desorbed with desorbing agents such as organic solvents (MeOH and Na_2EDTA) and inorganic solvents (HCl, H_2SO_4, HNO_3 and NaOH). The whole desorption process lasted for 4 h (Ding et al., 2023; Hu et al., 2024). In addition,

the possibility of recovering 0.125Fe@LBC-800 by degrading SMZ at different pyrolysis temperatures (300 ℃, 350 ℃, 400 ℃, 450 ℃, and 500 ℃) and pyrolysis times (30 min, 60 min, and 90 min) in a N_2 atmosphere was also investigated.

Text S4. Statistical analysis

The SMZ adsorption capacity and removal efficiency (R, %) were calculated using Eq. (S1) and Eq. (S2), respectively:

$$q_t = \frac{(C_0 - C_t)V}{m} \quad (S1)$$

$$R = \frac{C_0 - C_t}{C_0} \times 100 \quad (S2)$$

where C_0 (mg/L) and C_t (mg/L) represent the initial concentration and solution concentration at adsorption time t (min), respectively. q_t (mg/g) represents the adsorption capacity at adsorption time t (min). V (L) and m (g) represent the SMZ solution volume and the mass of the adsorbent, respectively. R (%) represent the removal efficiency.

To further investigate the adsorption kinetics, four commonly used models (pseudo-first-order, pseudo-second-order, intraparticle diffusion, and Elovich equations) were employed. Their specific equations are provided in Eq. (S3)−(S6):

$$q_t = q_e * (1 - e^{-k_1 t}) \quad (S3)$$

$$\frac{t}{q_t} = \frac{1}{k_2 {q_e}^2} + \frac{t}{q_e} \quad (S4)$$

$$q_t = k_p t^{\frac{1}{2}} + C \quad (S5)$$

$$q_t = \left(\frac{1}{\beta}\right) * (1 + \alpha * \beta * t) \quad (S6)$$

Here, where k_1 and k_2 are the equilibrium rate constants of the pseudo-first-order and

pseudo-second-order equations, respectively. q_e and q_t represent the adsorption capacity of SMZ at equilibrium and time t, respectively. k_1, k_2, and q_e can be calculated from the equation. k_p and C represent the intraparticle diffusion rate constant and the thickness of the boundary layer, respectively (Liu et al., 2017). Additionally, for the Elovich equation, α is the initial sorption rate (mg/(g·min)), whereas β is the Elovich constant associated with the adsorption process (mg/g) (Inyang et al., 2016).

The experimental data were analyzed via the Langmuir and Freundlich isotherm models, and the formulas of the two models are shown in Eqs. (S7) and (S8), respectively:

$$q_e = \frac{k_L q_m C_e}{1 + k_L C_e} \quad (S7)$$

$$lnq_e = \frac{1}{n} lnC_e + lnk_F \quad (S8)$$

Here, q_e represents the adsorption capacity of SMZ, and C_e represents the concentration of SMZ at equilibrium. q_m is the maximum adsorption capacity of the Langmuir isotherm. k_L is the Langmuir adsorption constant, which is related to the affinity of the adsorption rate and the energy of adsorption. k_F is Freundlich adsorption constant.

Text S5. Desorption and regeneration experiments

The regeneration performance of Fe@LBC-800 was evaluated by desorbing SMZ at a solid/liquid ratio of 1:1 (mg/mL) at 35°C and 180 rpm(Hu et al., 2024). Specifically, 0.125Fe@LBC-800 was desorbed with desorbing agents such as organic solvents (MeOH and Na_2EDTA) and inorganic solvents (HCl, H_2SO_4, HNO_3 and NaOH). The whole desorption process lasted for 4 h (Ding et al., 2023; Hu et al., 2024). In addition,

the possibility of recovering 0.125Fe@LBC-800 by degrading SMZ at different pyrolysis temperatures (300 ℃, 350 ℃, 400 ℃, 450 ℃, and 500 ℃) and pyrolysis times (30 min, 60 min, and 90 min) in a N_2 atmosphere was also investigated. The desorption efficiency of SMZ from used 0.125Fe@LBC-800 was calculated using Eq. (S9):

$$DE = \frac{C_d \times V_d}{q_e \times m} \times 100 \qquad (S9)$$

where C_d (mg/L) is the SMZ concentration in the desorption solution, V_d (L) is the volume of desorption solution, q_e (mg/g) is the equilibrium adsorption capacity before desorption, m (g) is the mass of the adsorbent, and DE (%) is desorption efficiency.

Text S6. Sample digestion procedure of Fe@LBC

The Fe content in 0.125Fe@LBC-800 was determined using inductively coupled plasma-optical emission spectrometry (ICP-OES, iCAP PRO, Thermo Fisher Scientific, USA). Prior to analysis, the samples were prepared following an acid digestion procedure (Oliveira et al., 2026). Briefly, 0.1 g of the biochar sample was mixed with 2.0 mL HNO_3 (3.5 mol/L) and 1 mL H_2O_2 in a digestion vessel. The mixture was heated at 280 ℃ for 60 min until a clear solution was obtained. After cooling, the digest was transferred to a volumetric flask and diluted to the mark with ultrapure water. The resulting solution was further diluted as necessary to bring the analyte concentration within the calibration range. Blank and quality control samples were prepared using the same procedure.

Table S1 Element proportion of LBM, LBC-800, used LBC-800, 0.125Fe@LBC-600, 0.125Fe@LBC-800, used 0.125Fe@LBC-800.

Material	C (%)	O (%)	S (%)	N (%)	Fe (%)	(O+N)/C
LBM	55.4	38.7	3.9	2.0	< 0.1	0.73
LBC-800	85.9	12.9	< 0.1	1.2	< 0.1	0.16
Used LBC-800	86.1	11.0	0.2	2.7	< 0.1	0.16
0.125Fe@LBC-800	89.6	6.9	< 0.1	2.3	1.2	0.10
Used 0.125Fe@LBC-800	87.0	9.2	0.4	3.1	0.3	0.14

Table S2 Elovich kinetic model parameters for the adsorptive removal of SMZ.

	Elovich kinetic model		
	α, mg/(g·min)	β, mg/g	R^2
LBC-800	0.2439	0.1769	0.9363
0.125Fe@LBC-800	50.0291	0.1591	0.9273

Table S3 Comparison of Fe-modified biochar adsorbents for sulfonamide removal.

Material	Biochar precursor	Morphology of Fe	Pollutant	q_m (mg/g)	Equilibrium Time (min)	pH Dependence	Ref.
Iron-modified biochar	Wheat straw	Fe_3O_4 and Fe^0	Sulfadiazine	49.07	540	pH-dependent, optimum pH 3.0	(Yan et al., 2022)
Magnetic biochar	Bagasse	Fe_3O_4, Fe_2SiO_4 and Fe^0	Sulfamethoxazole	187.31	240	pH-dependent, optimum pH 3.5−4.0	(Zhang et al., 2020)
Fe_3O_4 coated with carbon	Glucose	Fe_3O_4	Sulfathiazole	0.10	1440	pH-dependent, optimum pH 4.8	(Bao et al., 2014)
Biochar-supported magnetic $CuZnFe_2O_4$ composite	Bamboo	$CuZnFe_2O_4$	Sulfamethoxazole	99.99	30	pH-dependent, optimum pH 3.0−6.0	(Heo et al., 2019)
Iron-nitrogen co-doped modified biochar	Palm fiber powder	γ-Fe_2O_3, Fe_3O_4 and Fe_3C	Sulfamethoxazole	42.90	480	pH-dependent, optimum pH 5.0	(Diao et al., 2022)
Amino CNTs/$CoFe_2O_4$	Carbon nanotube	$CoFe_2O_4$	Sulfamethoxazole	8.00	1440	pH-dependent, optimum pH 2.0	(Li et al., 2019)
Magnetic nanocomposites	2-aminoterephthalic acid	$FeCO_3$, Fe and Fe_3C	Sulfamethoxazole	~80.00	720	pH-dependent, optimum pH 2.0−3.0	(Ou et al., 2020)
Fe@LBC	Lignin	γ-Fe_2O_3	Sulfamethazine	39.87±0.15	180	No pH dependence (pH 3.0−9.0)	This work

q_m (mg/g): maximum adsorption capacity.

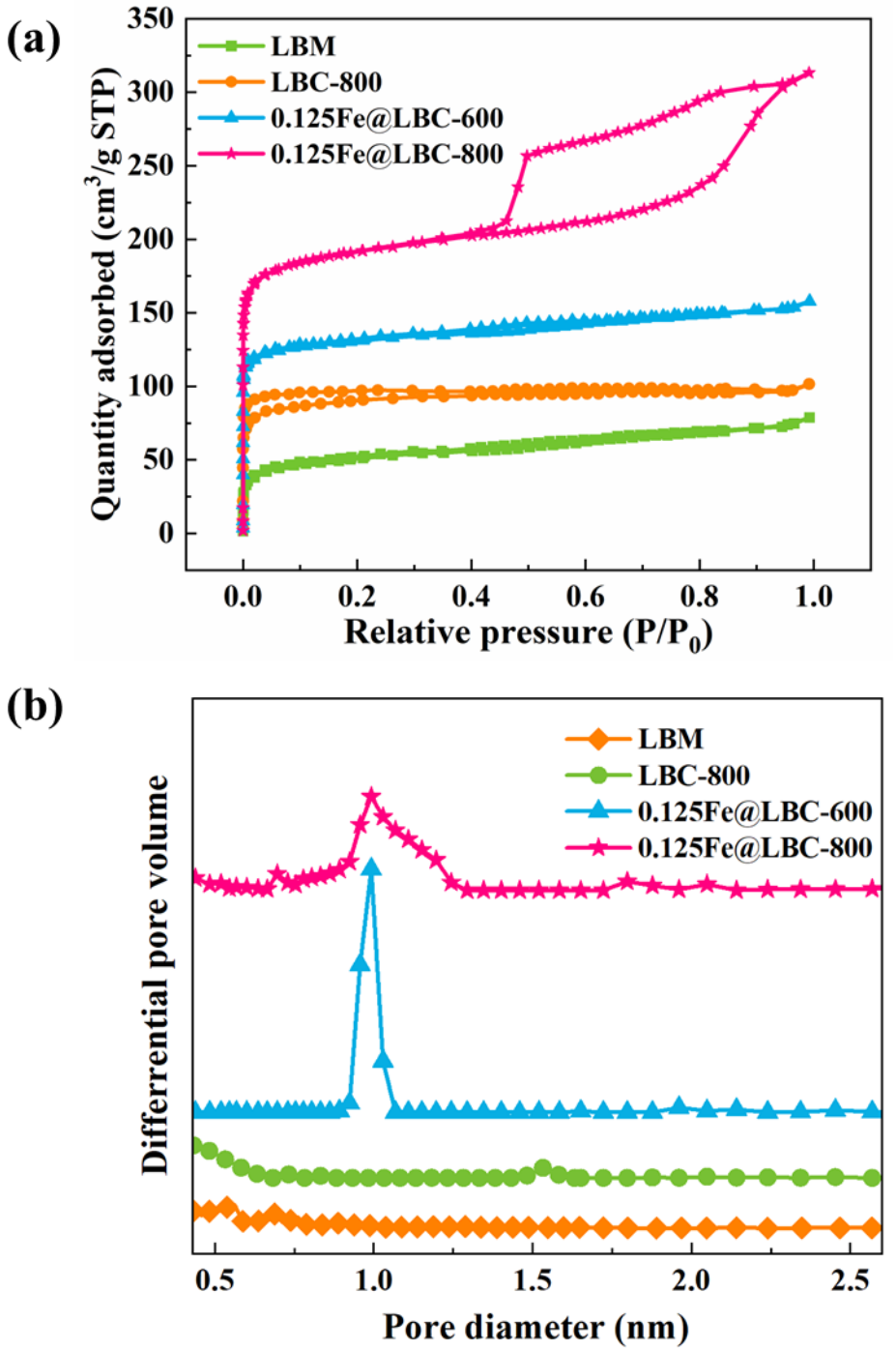

Fig. S1 The (a) nitrogen adsorption-desorption isotherms and (b) pore size distribution of LBM, LBC-800, 0.125Fe@LBC-600 and 0.125Fe@LBC-800.

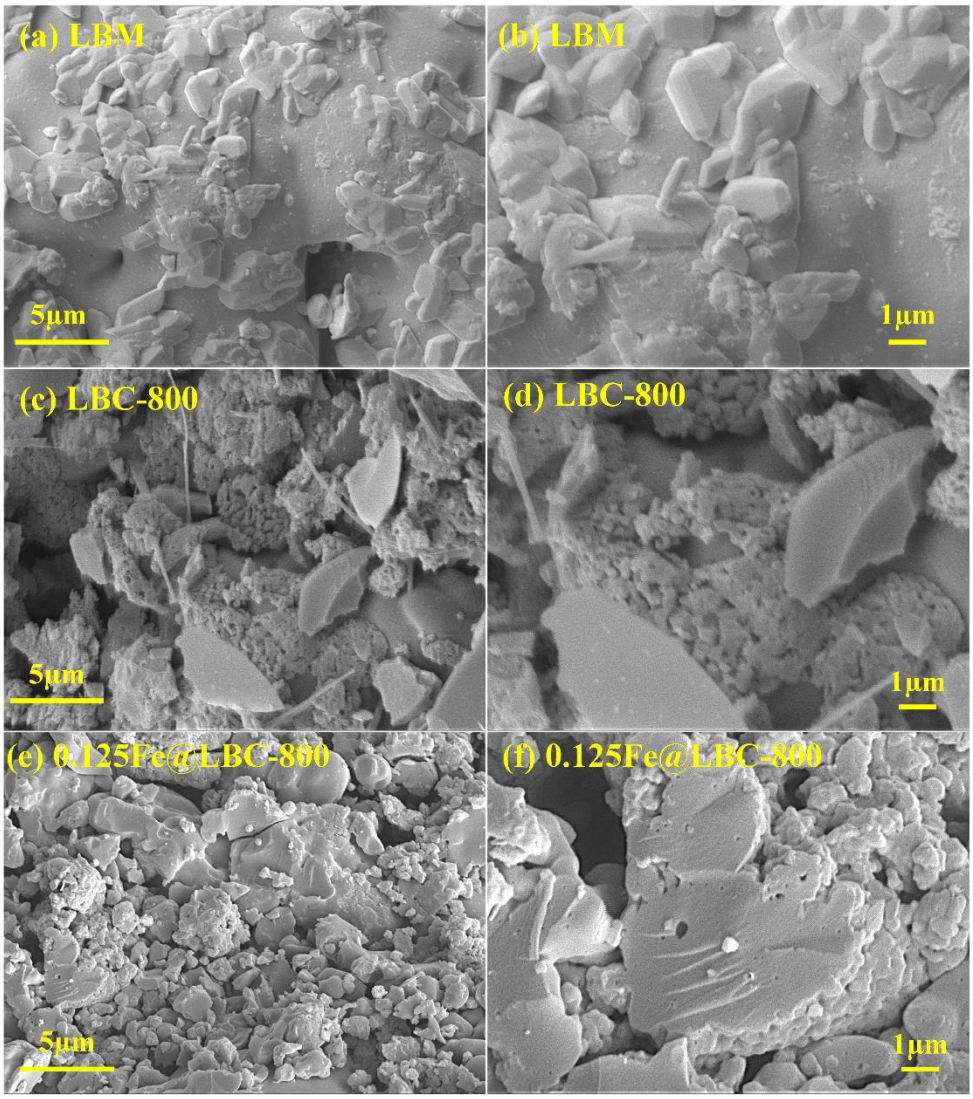

Fig. S2 The SEM images of (a, b) LBM, (c, d) LBC-800, (e, f) 0.125Fe@LBC-800.

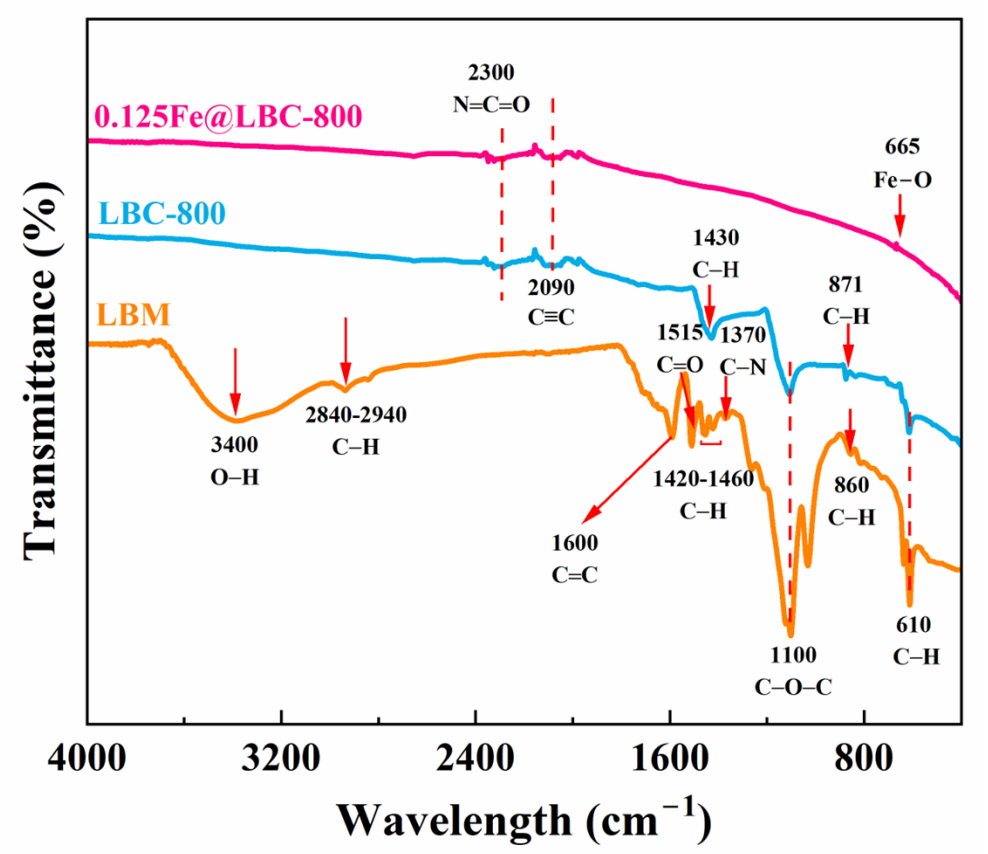

Fig. S3 FTIR spectroscopy analysis of LBM, LBC-800 and 0.125Fe@LBC-800.

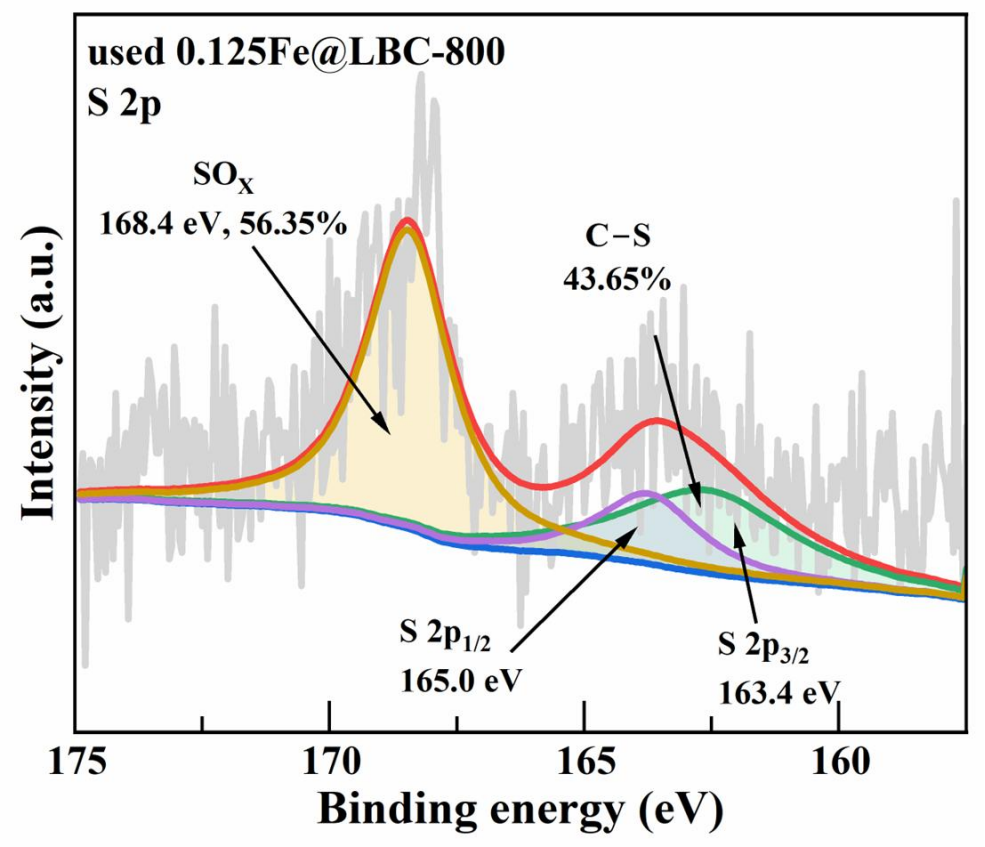

Fig. S4 XPS spectra of S 2p.

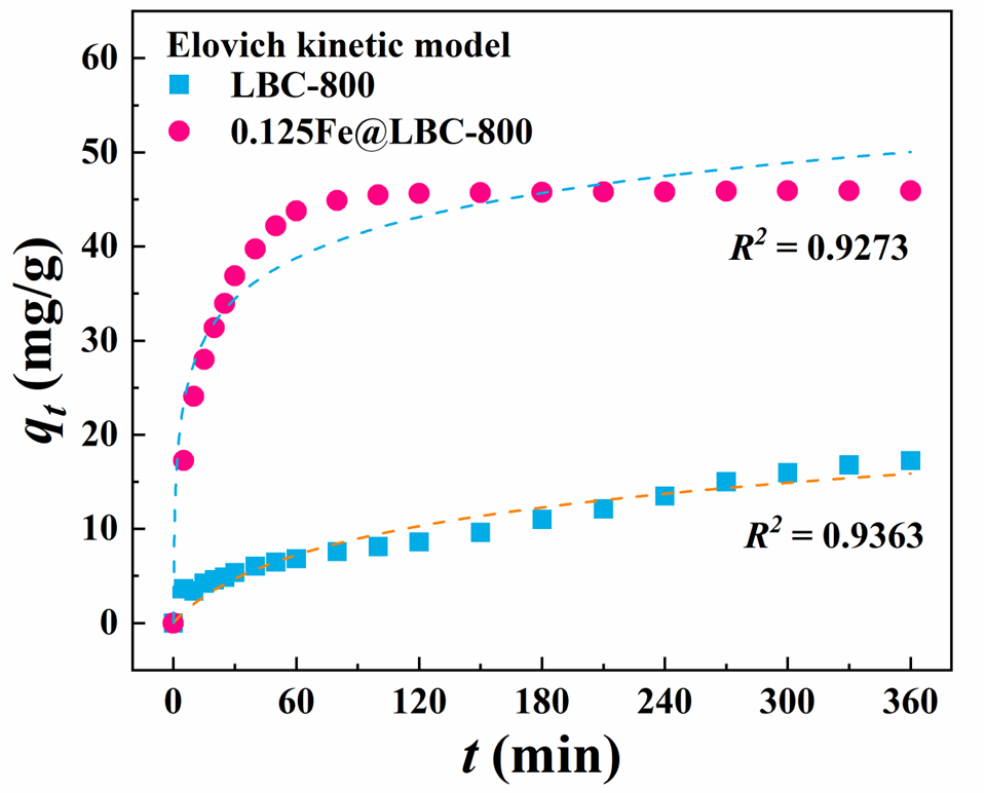

Fig. S5 Elovich kinetic model under the following conditions: 35 ℃, 0.5 g/L adsorbent, 20 mg/L initial SMZ concentration, and pH 7.0±0.1.

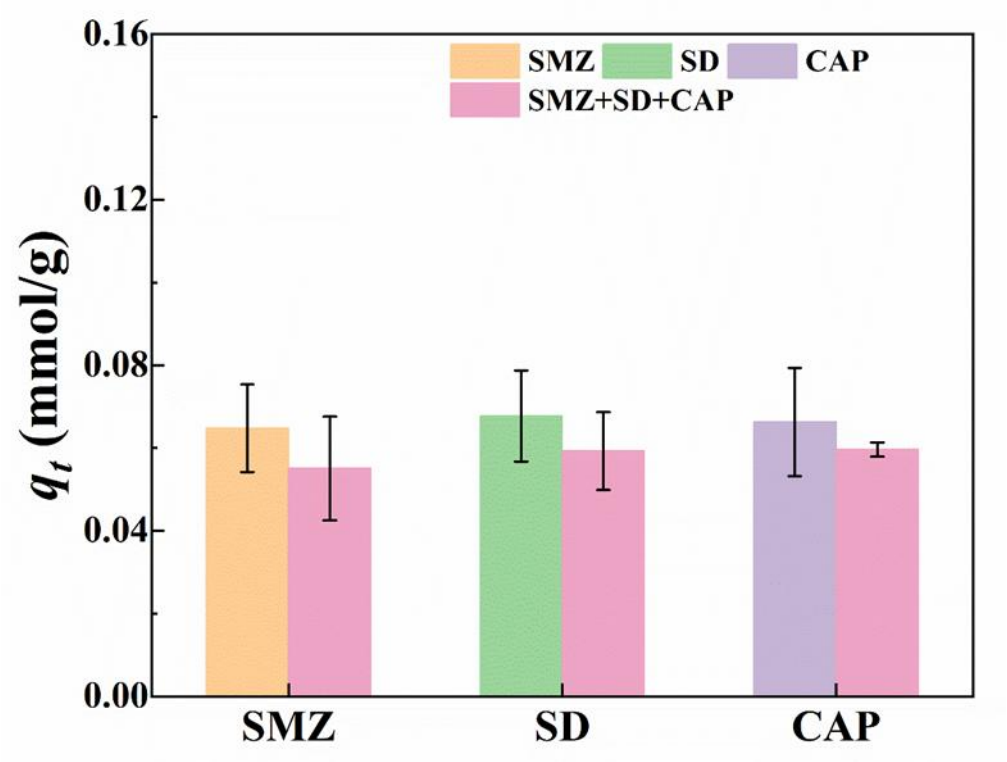

Fig. S6 Adsorption performance of LBC-800 toward SMZ, SD, and CAP under single and coexisting antibiotic systems.

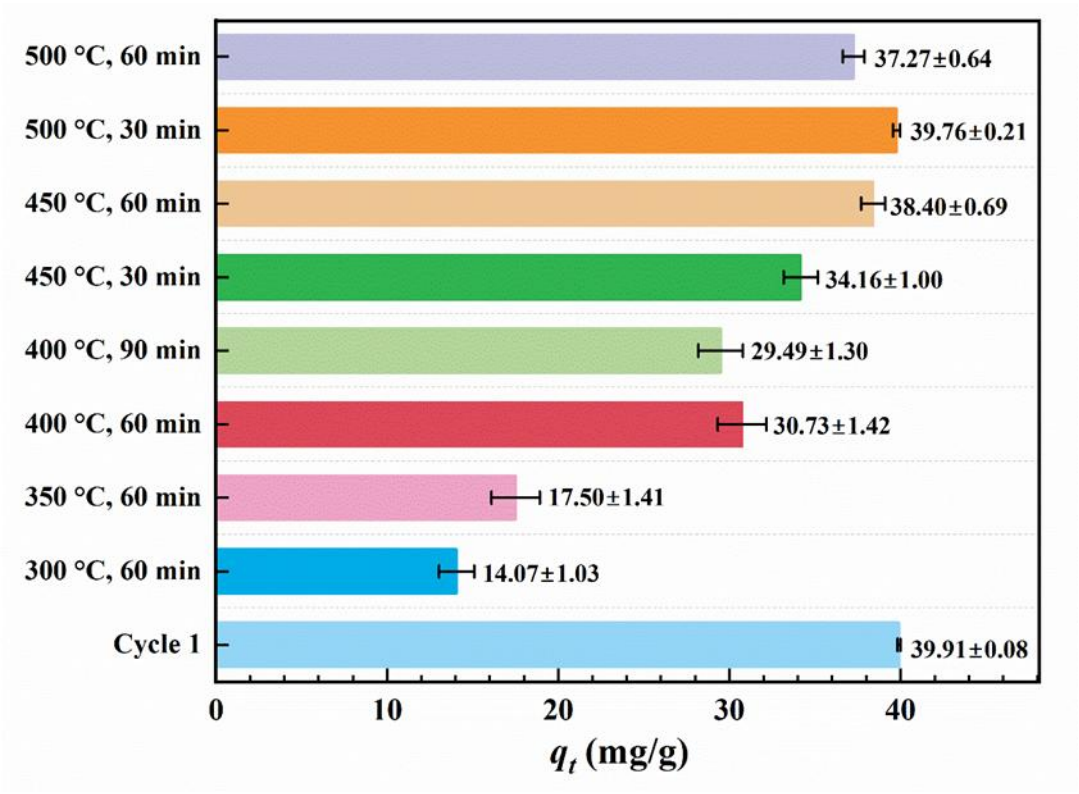

Fig. S7 Effect of calcination temperature and time on the regeneration and re-adsorption capacity of spent adsorbent.

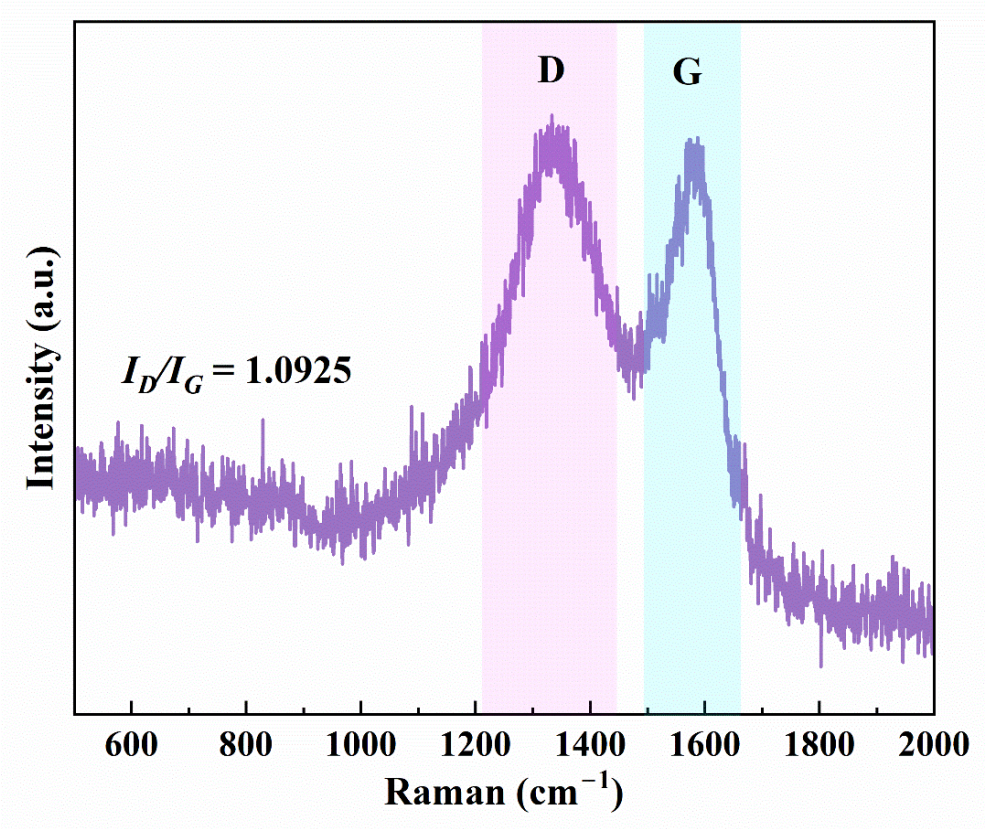

Fig. S8 Raman spectra of regenerated 0.125Fe@LBC-800 after adsorption-thermal regeneration.

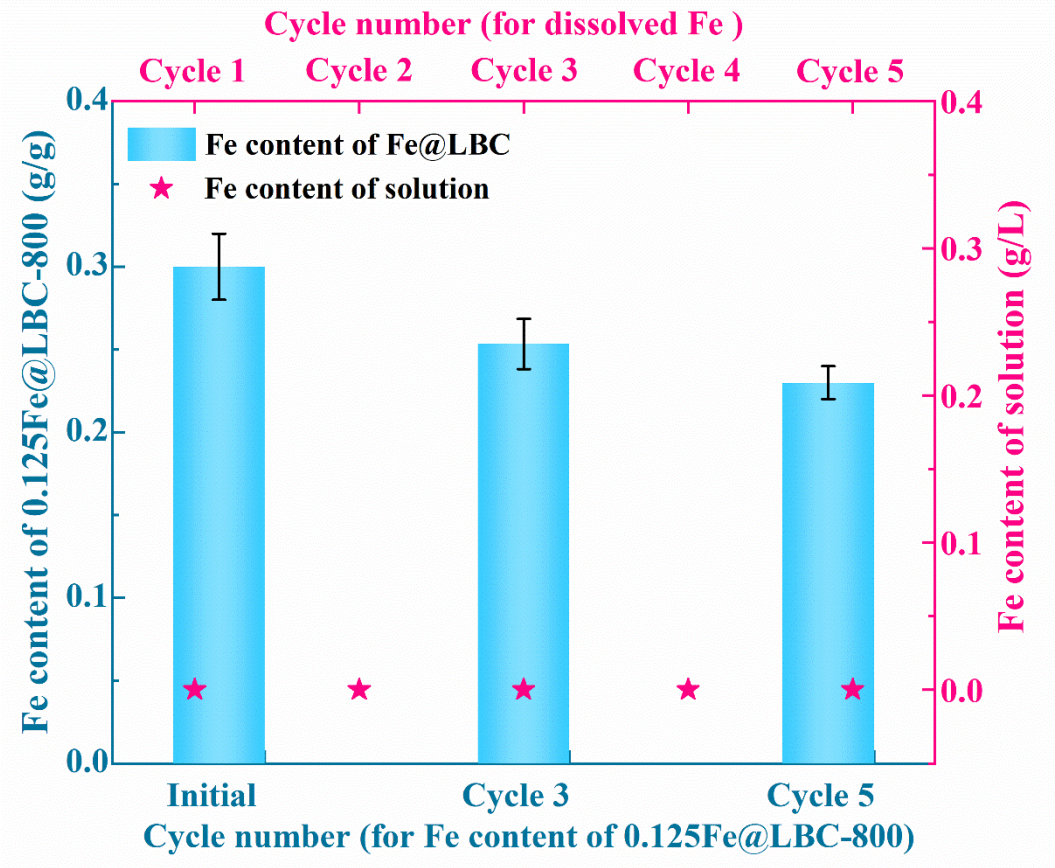

Fig. S9 Fe content in 0.125Fe@LBC-800 (bars) and dissolved Fe concentration (dots) as a function of cycle number.

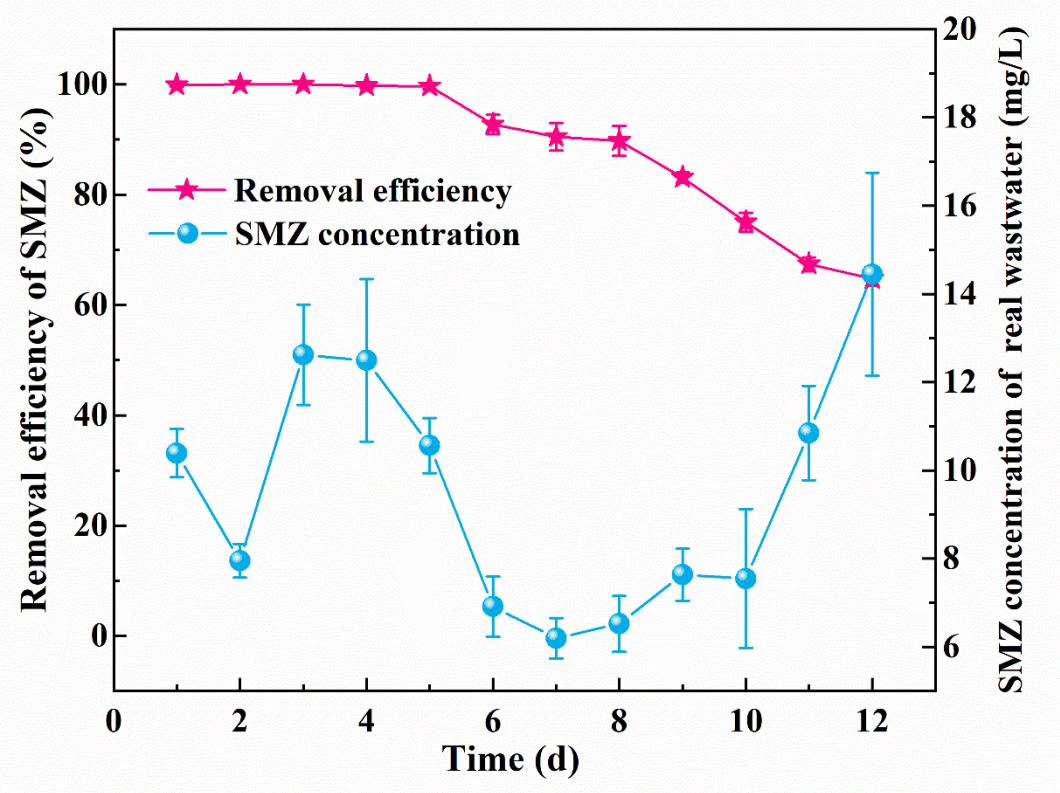

Fig. S10 Long-term SMZ removal by 0.125Fe@LBC-800 in real pharmaceutical wastewater over 12 days.

References

Bao X, Qiang Z, Chang J H, Ben W, Qu J (2014). Synthesis of carbon-coated magnetic nanocomposite (Fe_3O_4@C) and its application for sulfonamide antibiotics removal from water. Journal of Environmental Sciences, 26(5): 962-969

Diao Y, Shan R, Li M, Gu J, Yuan H, Chen Y (2022). Efficient adsorption of a sulfonamide antibiotic in aqueous solutions with N-doped magnetic biochar: Performance, mechanism, and reusability. ACS Omega, 8(1): 879-892

Ding H, Tong G, Sun J, Ouyang J, Zhu F, Zhou Z, Zhou N, Zhong M (2023). Regeneration of methylene blue-saturated biochar by synergistic effect of H_2O_2 desorption and peroxymonosulfate degradation. Chemosphere, 316: 137766

Heo J, Yoon Y, Lee G, Kim Y, Han J (2019). Enhanced adsorption of bisphenol A and sulfamethoxazole by a novel magnetic $CuZnFe_2O_4$-biochar composite. Bioresource Technology, 281: 179-187

Hu W, Niu Y, Shen T, Dong K, Wang D (2024). Magnetic biochar prepared by a dry process for the removal of sulfonamides antibiotics from aqueous solution. Journal of Molecular Liquids, 400: 124576

Inyang H I, Onwawoma A, Bae S (2016). The Elovich equation as a predictor of lead and cadmium sorption rates on contaminant barrier minerals. Soil and Tillage Research, 155: 124-132

Li S, Wang F, Pan W, Yang X, Ni J (2019). Molecular insights into the effects of Cu(II) on sulfamethoxazole and 17β-estradiol adsorption by carbon nanotubes/$CoFe_2O_4$ composites. Chemical Engineering Journal, 373: 995-1002

Liu F, Zhang W, Chen W, Wang J, Yang Q, Zhu W, Wang J (2017). One-pot synthesis of $NiFe_2O_4$ integrated with EDTA-derived carbon dots for enhanced removal of tetracycline. Chemical Engineering Journal, 310: 187-196

Lu T (2024). A comprehensive electron wavefunction analysis toolbox for chemists, Multiwfn. The Journal of Chemical Physics, 161(8): 082503

Oliveira E M, Ferreira E C, Neto J A G, Virgilio A (2026). Closed-vessel conductively heated digestion system with diluted nitric acid for the preparation of biomass and biochar samples. Talanta, 296: 128488

Ou Y, Yao L, Li Y, Bai C, Luque R, Peng G (2020). Magnetically separable Fe-MIL-88B_NH_2 carbonaceous nanocomposites for efficient removal of sulfamethoxazole from aqueous solutions. Journal of Colloid and Interface Science, 570: 163-172

Yan J, Zuo X, Yang S, Chen R, Cai T, Ding D (2022). Evaluation of potassium ferrate activated biochar for the simultaneous adsorption of copper and sulfadiazine: Competitive versus synergistic. Journal of Hazardous Materials, 424: 127435

Zhang R, Zheng X, Chen B, Ma J, Niu X, Zhang D, Lin Z, Fu M, Zhou S (2020). Enhanced adsorption of sulfamethoxazole from aqueous solution by Fe-impregnated graphited biochar. Journal of Cleaner Production, 256: 120662